

Journal of Materials Chemistry B

Accepted Manuscript



This is an *Accepted Manuscript*, which has been through the Royal Society of Chemistry peer review process and has been accepted for publication.

Accepted Manuscripts are published online shortly after acceptance, before technical editing, formatting and proof reading. Using this free service, authors can make their results available to the community, in citable form, before we publish the edited article. We will replace this *Accepted Manuscript* with the edited and formatted *Advance Article* as soon as it is available.

You can find more information about *Accepted Manuscripts* in the [Information for Authors](#).

Please note that technical editing may introduce minor changes to the text and/or graphics, which may alter content. The journal's standard [Terms & Conditions](#) and the [Ethical guidelines](#) still apply. In no event shall the Royal Society of Chemistry be held responsible for any errors or omissions in this *Accepted Manuscript* or any consequences arising from the use of any information it contains.

**Chitosan-*g*-oligo(epsilon-caprolactone) polymeric micelles:
Microwave-assisted synthesis and physicochemical and
cytocompatibility characterization**

Romina J. Glisoni^{1‡}, Silvina S. Quintana L^{2‡}, María Molina³, Marcelo Calderón³,
Albertina G. Moglioni² and Alejandro Sosnik^{5*}

¹NANOBIOTEC, University of Buenos Aires-National Science Research Council
(CONICET), Buenos Aires, Argentina

²IQUIMEFA, University of Buenos Aires-National Science Research
Council (CONICET), Buenos Aires, Argentina

³Institut für Chemie und Biochemie, Freie Universität Berlin, Berlin, Germany

⁴Laboratory of Pharmaceutical Nanomaterials Science, Department of Materials
Science and Engineering, Technion-Israel Institute of Technology, Haifa, Israel

[‡]Equally contributed to this work.

***Corresponding author:**

Prof. Alejandro Sosnik
Department of Materials Science and Engineering
De-Jur Building, Office 607
Technion-Israel Institute of Technology
Technion City
3200003 Haifa, Israel
Phone #: +972-077-887-1971
Emails: alesosnik@gmail.com, sosnik@tx.technion.ac.il

ABSTRACT

Aiming to produce mucoadhesive polymeric micelles for drug administration by mucosal routes, chitosan-*g*-oligo(epsilon-caprolactone) copolymers were synthesized by a microwave-assisted ring-opening polymerization of epsilon-caprolactone using chitosan as macroinitiator and methanesulfonic acid as solvent, catalyst and protecting group of the amine moieties. The reaction was conducted under very mild conditions and completed within 10 min with a monomer conversion above 90%. The grafting of oligo(epsilon-caprolactone) blocks to the free hydroxyl groups of chitosan was confirmed by ATR/FT-IR, ¹H- and ¹³C-NMR, WAXD and thermal analysis (TGA/DSC). The molecular weight of the synthetic hybrid copolymers was determined by GPC and MALDI-ToF mass spectrometry. Polymeric micelles obtained by the solvent diffusion/evaporation method showed spherical shape (TEM and AFM), sizes between 111-154 nm and highly positive zeta-potential (>+50 mV) (DLS). In addition, they displayed good cell compatibility in the human lung adenocarcinoma epithelial line A549 and were readily up-taken by the cervical cancer cell line HeLa. Results of the encapsulation of the antituberculosis drug rifampicin showed better performance than other nanocarriers previously investigated (e.g., cyclodextrins). Moreover, the micelles conserved the mucoadhesiveness displayed by pristine chitosan and, in addition, are expected to transiently open tight cell junctions and lead to more prolonged residence times in mucosal tissues and greater drug bioavailability.

KEYWORDS: Chitosan-*graft*-oligo(epsilon-caprolactone) copolymers; microwave-assisted ring-opening polymerization; mucoadhesive polymeric micelles; rifampicin encapsulation.

1. INTRODUCTION

Polymeric micelles (PMs) represent one of the most versatile nanotechnology platforms to improve the performance of poorly-water soluble drugs.¹ PMs are formed by the self-assembly of copolymeric amphiphiles above the critical micellar concentration (CMC) and display two primary domains, a hydrophobic core and a hydrophilic corona. Due to the great flexibility to tailor their molecular weight, hydrophilic-lipophilic balance (HLB), size, architecture, surface chemistry and shape, PMs can fit the encapsulation of diverse poorly water-soluble drugs. Despite their potential, a few PMs reached the clinical stages and all of them for the therapy of cancer by the intravenous route. More recently, the potential of these nanocarriers for mucosal drug administration has been highlighted.^{2,3} Our research group and others have comprehensively explored the administration of PMs by non-parenteral routes.⁴⁻¹⁰

The main drawbacks of PMs for non-parenteral drug delivery are the weak interaction with mucosa and the associated short residence time in mucosal tissues. To extend the application of PMs, the development of mucoadhesive PMs is currently under investigation. In this framework, the hydrophobization of polysaccharide molecular templates is one of the most promising approaches.¹¹

Chitosan (CS), a product of the partial or full deacetylation of chitin, is formed by two repeating units of β -(1 \rightarrow 4)-linked D-glucosamine (deacetylated unit) and *N*-acetyl-D-glucosamine. Owing to good biocompatibility, biodegradation and mucoadhesiveness it has become one of the most popular natural biomaterials in drug delivery.^{12,13} CS establishes a combination of ionic, hydrogen and hydrophobic bonds with the negatively-charged mucin and also transiently opens tight junctions in the intestinal epithelium increasing the drug absorption extents. Different chemical

pathways have been explored to graft hydrophobic blocks and confer amphiphilicity to the polysaccharide backbone. Most of them indiscriminately modify both pendant hydroxyl and amine groups. However, to maximize mucoadhesiveness, amine moieties should remain largely intact and thus different protection methods have been proposed. For example, the initial amidation with phthaloyl chloride^{14,15} and later deprotection under relatively mild conditions.¹⁶ The main drawback of this approach is the introduction of toxic aromatic residues that might be incompatible with biomedical uses and the demand of profuse purification steps. The CS salt produced with methanesulfonic acid (MSA) is a simple and reversible protection method¹⁷ that enables graft polymerization reactions of CS in homogeneous water-free media.¹⁸ MSA is a pharmaceutical excipient approved for parenteral administration and used to produce salts, namely methanesulfonates or mesylates, of poorly-water soluble drugs and increase their aqueous solubility.¹⁹

Poly(epsilon-caprolactone) (PCL) is a biocompatible polyester with higher hydrophobicity and slower hydrolysis rate than poly(lactic acid) polymers that due to the ability to sustain the release of both hydrophilic and hydrophobic drugs has gained a prominent place in the development of drug delivery systems.²⁰

Aiming to produce mucoadhesive PMs, in this work, we investigated the grafting of short PCL blocks to the side-chain of a low molecular weight CS precursor by a fast microwave-assisted ring opening polymerization of epsilon-caprolactone (CL) in MSA medium. The reaction was completed within 10 min and the monomer conversion was high. Spherical PMs with sizes in the 111-154 nm range and highly positive zeta-potential were obtained, these findings being consistent with the availability of free protonated amine groups. In addition, micelles displayed good cell compatibility, were up-taken by a phagocytic cell line and encapsulated the model

drug rifampicin to a greater extent than other popular drug nanocarriers. Overall results support the potential of this nanotechnology platform for the improved administration of drugs by the mucosal routes.

2. EXPERIMENTAL SECTION

2.1. Materials

Low molecular weight (M_w) CS (degree of deacetylation of 75-85%; viscosity of 20-200 cP, 1% w/v in 1% acetic acid solution by Brookfield method at 25°C), CL and MSA were supplied by Sigma-Aldrich (St. Louis, MO, USA). CL and MSA were dried with activated molecular sieves 3A (Sigma-Aldrich) at least 24 h before use. Rifampicin (RIF, 98.2% purity) was purchased from Parafarm® (Buenos Aires, Argentina) and used as received. All the other solvents were of analytical or spectroscopic grade (Sintorgan, Buenos Aires, Argentina) and used without further purification.

2.2. Methods

2.2.1. Synthesis of CS amphiphiles. The microwave-assisted graft polymerization of CL was conducted in a monowave 300 high performance microwave reactor (Anton Paar® GmbH, Graz, Austria). CS:CL weight feeding ratios of 1:8; 1:12; 1:16 and 1:24 were used to obtain CS-*g*-oligo(CL) copolymers with growing molecular weight and CL content (**Table 1**). Briefly, dry CS (0.5 g) was placed in a dried glass reactor and dissolved in dry MSA (7.5 mL), followed by the injection of a certain amount of CL (4-12 g for the different copolymers). Then, the reactor was irradiated at (i) 45°C (5 min) and (ii) 70°C (5 min); these conditions were identical for all the derivatives. Reaction crudes were thoroughly dialyzed against distilled water (regenerated cellulose dialysis membranes; MWCO of 3500 g/mol, Spectra/Por® 3

nominal flat width of 45 mm, diameter of 29 mm, and volume/length ratio of 6.4 mL/cm; Spectrum Laboratories, Inc., Rancho Dominguez, CA, USA) for 72 h, frozen (-80°C, 24 h) and freeze-dried (48 h). CS-*g*-oligo(CL) copolymers synthesized with CS:CL weight ratios of 1:8, 1:12, 1:16 and 1:24 are named CS-CL8, CS-CL12, CS-CL16 and CS-CL24, respectively. The synthesis of fluorescent CS-CL8 copolymer used in cell uptake assays was carried out by reacting 0.2 g of the copolymer with 4.5 mg of fluorescein isothiocyanate (Isomer I, FITC, Sigma-Aldrich) in *N,N*-dimethylformamide (DMF) (10 mL) at room temperature (12 h) protected from light as reported elsewhere.²¹ Then, the product was dialyzed (24 h), frozen and freeze-dried (48 h).

2.2.2. Characterization of CS-*g*-oligo(CL) copolymers. The different products were fully characterized and compared to pristine CS and when relevant to poly(epsilon-caprolactone)diol (PCL, M_w of 40 kg/mol) synthesized following a previous microwave-assisted technique.²²

Attenuated Total Reflectance/Fourier Transform-Infrared Spectroscopy (ATR/FT-IR). ATR/FT-IR spectra of CS-CL8, CS-CL12, CS-CL16 and CS-CL24 were recorded in a Nicolet 380 spectrometer (Avatar Combination Kit, Smart Multi-Bounce HATR with ZnSe crystal 45° reflectance, Thermo Scientific, Madison, WI, USA) from 4000 to 600 cm^{-1} (32–64 scans with a resolution of 4 cm^{-1}) at room temperature. For this, powders were mounted on the ATR crystal-ZnSe metal plate (45° angle) and spectra obtained using the Thermo Scientific OMNIC 8 spectrum software (Thermo Scientific).

Proton and carbon Nuclear Magnetic Resonance Spectroscopy (NMR). ^1H - and ^{13}C -NMR spectra of the different copolymers were recorded in a 500-MHz Bruker® Avance II High Resolution spectrometer (^1H - at 500.13 MHz and ^{13}C -NMR at 125.77

MHz) and Bruker TOPSPIN 2.1 software (Bruker BioSpin GmbH, Rheinstetten, Germany) using acetone- d_6 (Sigma-Aldrich) as solvent and 2% w/v solutions. Chemical shifts are reported in ppm using tetramethylsilane (TMS) as internal standard. The experimental average number of CL units per glucosamine unit in the graft copolymer (CL_n) was calculated from $^1\text{H-NMR}$ spectra according to Equation 1²³

$$CL_n = (A_{\text{PCL}}/A_{\text{CS}})/2 \quad (1)$$

Where A_{PCL} represents half of the integration area of $-\text{CH}_2$ protons of oligo(CL) at 2.30 ppm and A_{CS} is the integral area of the CS protons at 3.89 ppm.

Molecular weight. The molecular weight of the copolymers was determined using two complementary methods.

(i) *Matrix-assisted laser desorption/ionization-Time-of-Flight mass spectrometry (MALDI-TOF MS).* The mass spectral data of the graft copolymers was obtained using a Ultra Flex II MALDI-TOF (Bruker Daltonik GmbH, Bremen, Germany) equipped with a pulsed nitrogen laser, operating at a wavelength of 337 nm in reflectron mode, using 2,5-dihydroxybenzoic acid as matrix. Copolymers were dissolved in chloroform (10 $\mu\text{g/mL}$), mixed with the matrix (1 mg) dissolved in acetonitrile:water (3:2, v/v) in 1:1 (v/v) ratio, deposited onto a ground steel plate (Bruker Daltonics GmbH) and slowly dried to allow matrix crystallization.²⁴ MALDI-TOF MS spectra were recorded and the intensity represented as a function of the m/z in the range between 2000 and 60,000 g/mol using Bruker Daltonics Flex Analysis software (Bruker Daltonics GmbH) and calibrated by using commercial proteins (angiotensin, neurotensin insulin), and β - and γ -cyclodextrins as external standards.

(ii) *Gel permeation chromatography (GPC)*. Number- and weight-average molecular weights (M_n and M_w , respectively) and molecular weight distribution (defined M_w/M_n) were determined by analytical GPC using an Agilent 1100 Series HPLC System (Agilent Technologies, Santa Clara, CA, USA) including a refractive index detector.²⁵ Polystyrene standards were used for M_w calibration and the calculation done with Win-GPC Software. The measurements were run in tetrahydrofuran (THF) as eluent (flow of 1 mL/min) at 20°C using an array of Suprema Lux 100, Suprema 1000 and Suprema Lux 3000 columns (8 x 300 mm, polystyrene particle size of 10 μ m, Knauer Wissenschaftliche Geräte GmbH, Berlin, Germany).

Thermal analysis. The thermal behavior of the different copolymers was analyzed employing a TG-DSC SDT Q600 V8.1 simultaneous thermal analyzer using the Universal Analysis Software V4.2E (TA Instruments; New Castle, DE, USA) under dry N₂ atmosphere (flow of 100 mL/min) and In as standard. Dry samples (2.0-2.5 mg) were sealed in 40 μ L Al-crucibles pans and subjected to three consecutive thermal treatments at a heating/cooling rate of 10°C/min: (i) 25 to 100°C (first heating ramp to erase the thermal history), (ii) 100 to 0°C (cooling ramp) and (iii) 0 to 500°C (second heating ramp). The melting temperature (T_m) of native and graft copolymers and the enthalpy involved in each transition (ΔH_m) were calculated from the endothermic peaks, registered during the second heating ramps (see above). ΔH_m values were normalized to the PCL content of each copolymer. The remaining weight of sample (expressed in %) in the second heating ramp was also recorded.

Powder wide-angle X-ray diffraction (WAXD). The crystallinity of the different copolymers was analyzed by WAXD in an Empyrean Diffractometer (PANalytical, Almelo, Netherlands) using Ni-filtered Cu radiation generated at 40 mA and 40 kV.

The experimental data were collected between 0° and 60° at a scanning rate of 2°/min.

2.2.3. Preparation of RIF-free and RIF-loaded PMs. Drug-free PMs were prepared by the co-solvent diffusion/evaporation method. Briefly, copolymers (0.1 g) were dissolved in pure acetone and added drop wise (flow of 20 mL/h) to water (10 mL; Simplicity® Water Purification System, Millipore, Billerica, MA, USA; pH = 5.8) under mechanical stirring (three-blade propeller, 1060 RPM) using a programmable syringe infusion pump (PC11UB, APEMA, Buenos Aires, Argentina), at room temperature.²⁶ Mechanical stirring was continued under the same conditions for 1.5 h after the end of the addition to ensure the complete elimination of acetone.²⁷ Resulting aqueous dispersions were centrifuged (12,000 RPM; 15 min) with a Centrifuge 5810 R (Eppendorf AG, Hamburg, Germany) and filtered through clarifying filters (0.45 µm; GE nitrocellulose mixed esters membrane, Osmonics Inc., Minnesota, MN, USA).

To prepare RIF-loaded PMs, the procedure was similar to the previously described though with the addition of 10 mg/mL of RIF to the organic phase containing the copolymer. The drug payload into PMs was determined using UV-Visible spectroscopy ($\lambda_{\text{max.}} = 340 \text{ nm}$, CARY (1E) UV-Visible Spectrophotometer Varian, Palo Alto, CA, USA) at room temperature, after the appropriate dilution in DMF. A calibration curve of RIF in DMF covering the range between 5 and 50 µg/mL ($R^2 > 0.999$) was used. Copolymer solutions in DMF were used as blank. The percentage of RIF loading (%RIF) in the different micellar systems was calculated according to Equation 2

$$\%RIF = C_e / (C_e + C_p) \times 100 \quad (2)$$

Where experimental RIF cargo (C_e) is the concentration of RIF in PMs of a certain copolymer concentration (C_p), both values being expressed in mg/mL.

In addition, the encapsulation efficiency (%*EE*) of the PMs was determined according to Equation 3

$$\%EE = (C_e/C_t) \times 100 \quad (3)$$

Where C_t is the theoretical RIF cargo.

Finally, solubility factors (f_s) were calculated according to Equation 4

$$f_s = S_{PM}/S_{water} \quad (4)$$

Where S_{PM} and S_{water} are the apparent solubility of RIF in the corresponding PMs and the experimental intrinsic solubility in water determined at the time of the experiments (2.13 mg/mL), respectively, at 25°C. All the results were expressed as mean \pm S.D. of three independent samples prepared under identical conditions.

2.2.4. Characterization of the micellization process. Stock aqueous solutions (1% w/v) of the copolymers were diluted (0.0001–1% w/v) and stabilized at 37°C for at least 24 h. Refractive indices and viscosities for these measurements were between 1.333–1.350 and 0.6855–0.6875 cP, respectively (37°C). The intensity of the scattered light (DCR) expressed in kilo counts per second (kcps) was measured by Dynamic Light Scattering (DLS, Zetasizer Nano-ZS, Malvern Instruments, Malvern, UK) provided with a 4 mW He-Ne laser ($\lambda = 633$ nm), a digital correlator ZEN3600 and a Non-Invasive Back Scatter (NIBS[®]) technology (37°C) and plotted as a function of the copolymer concentration (% w/v). Measurements were carried out at a scattering angle of 173° to the incident beam and data were analyzed using CONTIN algorithms (Malvern Instruments). Data for each single specimen was the result of at least six runs. The micellization was observed as a sharp increase in the scattering intensity and the intersection between the two straight lines corresponded to the CMC.²⁴

2.2.5. Size, size distribution and zeta potential. The hydrodynamic diameter (D_h), the size distribution (polydispersity index, PDI) and the zeta-potential (Z-potential) of RIF-free and RIF-loaded fresh PMs were determined using the Zetasizer Nano-ZS. For Z-potential, laser Doppler micro-electrophoresis is used. Values are expressed as mean \pm S.D. of three independent samples prepared under identical conditions. Data for each single specimen were the result of at least six runs.

2.2.6. Morphology of the micelles. The morphology of fresh RIF-free and RIF-loaded (1% w/v) PMs was visualized by transmission electron microscopy (TEM) (Electron microscope ZEISS EM109 TEM, Oberkochen, Germany) equipped with a Digital ES1000W Erlangshen™ 11 megapixel high-speed affordable CCD camera (Model 785, Gatan GmbH, München, Germany). For this, PMs suspensions (1% w/v, 30-50 μ L) were deposited on a carbon grid membrane coated with a hydrophilic acrylic resin, the excess of sample was soaked with filter paper and the grid covered with a drop of phosphotungstic acid (50 μ L, 2% w/v in deionized water) during 60 s. Then, grids were air-dried and analyzed. Analysis was conducted at 80 kV and room temperature and the diameter of PMs estimated using TEM AutoTune™ software (Gatan Digital Micrograph® software, Gatan GmbH).

The morphology study was complemented by atomic force microscopy (AFM) using tapping mode (Nano World tips, Non-Contact/Tapping Mode-Long Cantilever, NCL-W) with resonance frequency of 190 kHz and spring constant of 48 N m⁻¹ (NanoDevices, Digital Instruments, Veeco, Santa Barbara, CA, USA) in a MultiMode 8 AFM equipped with a Nanoscope V controller (Veeco).²⁵ For this, PMs aqueous solutions (2 mg/mL) were spin coated on a mica sheet at 90 rps and 5 min. Data were analyzed using NanoScope Analysis 1.3 software.

2.2.7. *In vitro* mucoadhesion. The mucoadhesion of the micelles *in vitro* was determined using the mucin method that is based on the growth of the micellar D_h as a result of the interaction and agglomeration in the presence of soluble mucin.^{28,29} Briefly, mucin aqueous solution (0.25 % w/v) was prepared overnight at room temperature. Then, fresh PMs (5 mL, 1 % w/v) were added to the mucin solution (5 mL), vortexed (30 s) and incubated for 12 h at 37°C. Measurements of D_h were carried out by DLS as described above. The mucoadhesion index (MI) was calculated according to Equation 5

$$MI = D_{h12}/D_{h0} \quad (5)$$

Where D_{h0} and D_{h12} are the D_h of particles before ($t = 0$ h) and after ($t = 12$ h) the incubation with mucin, respectively. Results were expressed as mean \pm S.D. of three independent samples prepared under identical conditions. Data for each single specimen were the result of at least six runs.

2.2.8. *Cytotoxicity and cellular uptake.* A human lung adenocarcinoma epithelial cell line (A549) and an epithelioid human cervix carcinoma cell line (HeLa) were obtained from American Type Culture Collection (ATCC, Manassas, VA, USA) and cultured in Dulbecco's Modified Eagle Medium (DMEM, Life Technologies Corp., Carlsbad, CA, USA) supplemented with 10% heat-inactivated fetal calf serum (FCS, Life Technologies Corp.) and 1% penicillin/streptomycin (PAN-Biotech GmbH, Aidenbach, Germany), respectively. All cells were maintained at 37°C in a humidified 5% CO₂ atmosphere and split 1:10 into fresh media every three-four days.

(i) *Cytotoxicity of RIF-free PMs.* *In vitro* cytotoxicity of the PMs was assessed using the trypan blue (Sigma-Aldrich) exclusion assay. For this, A549 cells were seeded at a density of 1×10^5 cells/mL in 6-well plates and culture medium (2 mL) ($t = 0$) and incubated for 14 h. Then, fresh 0.1% PMs in fresh full growth medium were added to

the cells and incubated for 8 and 24 h, at 37°C and 5% CO₂. After the incubation time, the medium was removed and the cells were washed with 5 mL PBS and then trypsinized by adding 500 µL of trypsin solution (0.25%, PAN-Biotech GmbH). Trypsinization was stopped with 500 µL full growth medium. The cell suspension (50 µL) mixed with trypan blue solution (50 µL, 0.4%) was transferred to a Neubauer chamber and the number of unstained (live) cells determined. Cell viability should be at least 95% for healthy log-phase cultures. The statistical analysis on data of viable cell concentrations (relative to untreated control cells) was performed by a two-way analysis of variance (ANOVA). The software used was GraphPad Prism version 5.01 for Windows (GraphPad Software Inc., San Diego, CA, USA).

(ii) *Cellular uptake.* The cellular uptake of RIF-free PMs was tested in a phagocytic cell line, HeLa. For microscopic studies, 1×10^5 cells/mL were initially seeded on cover slips in 6-well plates and grown overnight at 37°C and 5% CO₂. Then, 1.0, 0.5, 0.1 and 0.05 mL of FITC-labeled PMs (0.1% w/v) was added to the cells and incubated for 15 h. FITC-labeled dextran (FITC-dextran, average molecular weight of 20 kg/mol, Sigma-Aldrich) was used as control. Thereafter, the media was removed, the cells were washed three times with PBS and fixed with 10% Neutral Buffered Formalin (NBF) in PBS (20 min) at room temperature. Afterwards, the fixing solution was removed and cells permeabilized with 0.1% Triton X-100 in PBS (5 min). Cover slips were washed three times with PBS and incubated in the dark (30 min, 37°C) with approximately 200 µL of 4,6-diamidino-2-phenylindole (2.5 µg/mL, DAPI, Carl Roth GmbH, Karlsruhe, Germany). After three times washings with PBS, cover slips were dipped in water, mounted onto microscopy slides with ProTaq Mount Fluor (Quartett) and dried overnight at room temperature. Microscopic image acquisition was performed with a TCS SP8 confocal laser scanning microscope (Leica

Microsystems GmbH, Wetzlar, Germany) with a 63x oil immersion objective and LASAF software (Leica).

3. RESULTS AND DISCUSSION

3.1. The rationale

The potential of PMs as nano-drug delivery systems by non-parenteral routes relies on the ability to synthesize polymeric amphiphiles with a strong aggregation tendency at relatively low concentrations and that, at the same time, display a micellar corona that undergoes strong interaction with mucin, a negatively-charged glycoprotein that is the main component of mucosa. In this work, we investigated the hydrophobization of CS templates by means of a fast microwave-assisted ring-opening graft polymerization of CL under very mild temperature. Aiming to conduct the reaction under homogenous conditions and preserve amine groups that play a fundamental role in mucoadhesion mainly unreacted, MSA was used as solvent, catalyst and protecting group.

3.2. Microwave-assisted graft polymerization of CL on CS templates

The microwave-assisted ring opening polymerization of lactones has been proven more efficient and faster than the conventional thermal reaction.^{27,30,31} Due to the extremely low solubility of CS in non-aqueous solvents, traditional synthetic pathways employ aqueous or heterogeneous chemistry or, conversely, ionic liquids as solvent.³²

In this study, we report for the first time on the microwave-assisted graft polymerization of CL to the free hydroxyl groups of CS in the presence of MSA as both catalyst and solvent (**Figure 1**). This medium not only solubilized CS but also prevented the opening of the lactone ring by the amine groups due to the formation

of a stable methanesulfonate salt. Reactions were completed within 10 min and the monomer conversion was greater than 90%. In addition, yellowish precursor solutions turned into dark brown crudes that after profuse dialysis resulted in light brown powders probably due to some level of CS oxidation. The gradual increase of the CL feeding ratio in the reaction mixture was used to increase the M_w of the hydrophobic blocks and the lipophilicity of the copolymer (**Table 1**). In general, the reaction yield was in the 75-90% range, growing for higher CL feeding ratios due to a decrease of the amount of low M_w products lost in the dialysis step (**Table 1**). Finally, as opposed to pristine CS, copolymers were readily soluble in DMF, THF, dimethyl sulfoxide (DMSO) and acetone (up to 20 mg/mL) and slightly soluble in chloroform.

3.3. Chemical characterization of the copolymers

The grafting of oligo(CL) blocks was confirmed by various complementary methods.

3.3.1. ATR/FT-IR. ATR/FT-IR spectra of unmodified CS showed characteristic bands at 1660 and 1600 cm^{-1} that corresponded to the stretching vibrations of the carbonyl (C=O) and free amine groups, respectively (**Figure 2A**). These results indicated that in agreement with the supplier information, CS was not completely deacetylated. After grafting, clear CH stretching bands of methylene groups at 2865 cm^{-1} and C=O at 1726 cm^{-1} due to the incorporation of oligo(CL) blocks were apparent (**Figure 2B**). These results fitted the spectrum of pure PCL (**Figure 2C**). In addition, the intensity of the band of the hydroxyl groups of pristine CS at 3000-3500 cm^{-1} decreased significantly. Furthermore, the carbonyl band gradually grew with the CL feeding ratio from CS-CL8 to CS-CL24 (data not shown).

3.3.2. ^1H - and ^{13}C -NMR. To confirm the grafting of oligo(CL) blocks, the copolymers were thoroughly analyzed by NMR spectroscopy and compared to pristine CS and PCL. The ^1H -NMR spectrum of CS-CL8 showed peaks at 4.04, 2.30, 1.75-1.63 and

1.40 ppm that corresponded to the oligo(CL) chains (**Figure 3A**). In addition, characteristic H signals of CS were observed at higher fields. Finally, the presence of a peak in 3.07 ppm that corresponds to the methyl group of methylsulfonate indicated the conservation of the amine groups as the methansulfonate salt and the prevention of the amidation reaction due to the ring opening of CL by the amine moieties (**Figure 3A**). In general, by increasing the CL feeding ratio, longer oligo(CL) blocks were produced. This growth in the CL content was gradual though no linear and the decrease of the grafting rate suggested a relative decrease of the monomer conversion for higher CL feeding ratios. To determine the average number of CL units in the side-chain per *N*-glucosamine repeating unit in the CS backbone, the experimental values of CL_n were calculated. For CS-CL8, CS-CL12, CS-CL16 and CS-CL24, CL_n values gradually increase from 19.6 to 39.7 (**Table 1**). Finally, ^{13}C -NMR spectra of all copolymers presented peaks of C=O at 174.05-175.15 ppm and CH and CH₂ at 20-70 ppm that are characteristic of oligo(CL) blocks (**Figure 3B**). Overall, these results confirmed the good efficiency of the synthetic method.

3.4. Molecular weight of the copolymer

MALDI-TOF MS data showed three m/z populations with similar peak maxima (**Table 2**) as exemplified in **Figure 4A** for CS-CL8. On the other hand, the peak with the highest m/z maximum corresponded to the M_w and showed a slight increase in the distribution end set values from 5747 g/mol for CS-CL8 to 6658 g/mol for CS-CL24 as the CL feeding ratio increased (**Table 2**). GPC analysis revealed that even if the values were in the same order of magnitude, they were smaller than those measured by MALDI-TOF MS (**Table 2**, **Figure 4B**). These differences are reasonable considering the different principle used by both methods and the fact that GPC standards were of polystyrene. In addition, the molecular weight distribution

was estimated from M_w/M_n where values between 1.7 and 3.8 (**Table 2**) were consistent with the use of polymeric precursors obtained from natural sources that usually show intrinsic high molecular weight dispersions.³³

3.5. Thermal characterization of the copolymers

DSC was used to study the thermal transitions of the different copolymers. The T_m of pristine PCL (M_w of 40 kg/mol) was 64°C and the associated ΔH_m 72.3 J/g. The T_m of the oligo(CL) blocks in the different copolymers gradually increased from 50°C for CS-CL8 to 54°C for CS-CL24 (**Table 1, Figure 5**). A decrease of the T_m and the ΔH_m (57.1-70.8 J/g) with respect to pure PCL stemmed from the lower crystallinity of oligo(CL) blocks in the copolymers due to their fragmented nature that increase the number of terminal repeating units and thus reduce their crystallizability. To gain understanding on the effect of the graft polymerization on the thermal stability of CS, samples were also analyzed by TGA where the weight loss was monitored during a heating step up to 500°C. CS showed a sharp weight loss of 40-45% at approximately 300°C that corresponded to the thermal decomposition of the polysaccharide chain (**Figure 6**). Then, the weight loss was less pronounced. Pristine PCL displayed a moderate weight loss up to 350°C when the most significant degradation began. The thermal degradation of the copolymers was much slower, with a weight loss of only 10-20% up to 350°C and a faster one between 400-450°C. These results were consistent with the increase of the thermal stability of CS due to the grafting of oligoester blocks in the side-chain.^{34,35}

3.6. WAXD of the copolymers

Powder WAXD patterns were recorded to confirm the crystalline nature of oligo(CL) blocks in the copolymers. It is worth mentioning that as opposed to DSC, the thermal history of these samples was not erased. CS and pristine PCL showed patterns of

amorphous and semi-crystalline materials, respectively. All the copolymers displayed two strong diffraction signals at 2θ 21.5° and 23.7° characteristic of semi-crystalline PCL (**Figure 7**).³⁶ These findings were in good agreement with the thermal analysis that showed the crystalline nature of the grafted polyester chains, regardless of their relatively short length when compared to PCL.

3.7. Characterization of the micellization process

All the derivatives showed very low CMC values between 3.6 and 5.0 x 10⁻⁴% w/v (equivalent to 3.6-5.0 x 10⁻³ mg/mL) (**Table 3**). Even though values were very similar, the increase of the CL feeding ratio led to a slight increase of the CMC. These results were unexpected because usually, the more hydrophobic the copolymer the lower the CMC; greater CL feeding ratio resulted in higher CL_n values (**Table 1**). On the other hand, it points out that longer oligo(CL) blocks hindered the self-aggregation process, a phenomenon that has been reported for other amphiphiles based on PCL as the hydrophobic component.²⁶ This behavior should be considered at the time of optimizing the drug encapsulation properties.

3.8. Characterization of RIF-free micelles

RIF-free PMs in aqueous solution (1% w/v) displayed D_h in the 111-154 nm range, as measured by DLS (**Table 3**). In addition, very low PDI values (0.12-0.23) were indicative of unimodal size distributions for all of them. As expected, the increase of the CL feeding ratio resulted in a gradual increase of the micellar size due to the enlargement of the hydrophobic core. In addition, the Z-potential of all the micelles was highly positive, consistent with the presence of free amine groups in protonated form due to the formation of a methanesulfonate salt (**Table 3**). The spherical morphology of RIF-free PMs was confirmed by TEM and AFM (**Figure 8**). Moreover, the average sizes visualized by both microscopies (90 ± 8 and 115 ± 30 nm,

respectively) were in good agreement with DLS data (**Table 3**). Small differences were due to the flattening or shrinking of the PMs during sample preparation.

To investigate the mucoadhesive properties, RIF-free PMs were incubated with mucin solution and the size growth change due to agglomeration monitored by DLS. A priori, a size growth was anticipated due to the positively-charged surface of the PMs (see Z-potential results) and the negative nature of sialic acid residues in mucin. In this context, MI values were between 3.4 and 9.2 times, CS-CL16 micelles showing the highest agglomeration (**Table 3**); CS-CL24 was very unstable and tended to precipitate relatively fast. These results supported the conservation of free amine groups. Intriguingly, the gradual increase in the agglomeration extent for copolymers bearing increasingly longer oligo(CL) block from CS-CL8 to CS-CL16 suggested the involvement of hydrophobic interactions of oligo(CL) blocks with hydrophobic domains in mucin, as previously shown for PCL nanoparticles.³⁴ On one hand, oligo(CL) blocks are expected to form the micellar core and not being exposed at the surface to interact with mucin. On the other, PMs are dynamic systems in equilibrium with free copolymer molecules (known as unimers) and thus, the gradual formation of agglomerates of non-micellized copolymer molecules and mucin that contributes to the size growth could not be ruled out.

3.9. Encapsulation of RIF

RIF is one of the most potent and effective antituberculosis agents, though its oral bioavailability is challenged by a low aqueous solubility and chemical instability in the acid gastric medium.^{38,39} Furthermore, there is a growing interest in nano-encapsulating RIF for inhalation delivery to target the mycobacterium reservoir, alveolar macrophages.^{18,40,41} In this scenario, conferring mucoadhesiveness to the nanocarrier would prolong the residence time of the drug delivery system in the

lungs and sustain the release of the encapsulated cargo. Due to a peculiar combination of molecular features including bulkiness, amphotericity and amphiphilicity, RIF is hard to encapsulate within PMs and other nanocarriers.⁴² We were interested in evaluating the performance of CS-*g*-oligo(CL) PMs as a possible nanotechnology platform that would pave the way to a more efficient RIF nano-encapsulation. The encapsulation was possible in CS-CL8, CS-CL12 and CS-CL16 PMs (1% w/v), f_s average values being 1.7, 1.5 and 1.9, respectively (**Table 3**). %RIF and %EE values were 24-28% and 31-40%, for CS-CL8, CS-CL12 and CS-CL16 (**Table 3**). When the oligo(CL) chains increased in the graft copolymer, RIF-loading capacity and encapsulation efficiency seemed to increase slightly, although the trend was not clear (**Table 3**). Conversely, the encapsulation failed with CS-CL24 due to a fast precipitation of this very hydrophobic copolymer in aqueous medium immediately after addition of the organic solution to water during the production process (**Table 3**). RIF-loaded PMs retained the spherical morphology without any sign of drug crystallization in the core (**Figure 9**), as opposed to other PCL-containing micelles.²⁶ This encapsulation performance was similar to that of 1% flower-like PMs.²⁶ Moreover, PMs conserved the strong electropositive surface upon encapsulation (**Table 3**). Thus, mucoadhesiveness in mucosal epithelia are expected to prolong the residence time and increase the bioavailability of the cargo.

3.10. Cytocompatibility and cellular uptake

Mucoadhesive PMs are designed to deliver drugs by mucosal routes. Thus, initially we assessed the cytocompatibility of RIF-free PMs using in A549 cells, a lung epithelial cell line. This cell line is a valid *in vitro* model of the pulmonary epithelium that could be of relevance in the inhalatory treatment of tuberculosis. PMs showed good cell compatibility (between 70-90%) after 8 h of exposure with minimal

dependence of the oligo(CL) length (**Figure 10**). Longer exposure led to a slight decrease of the cell viability though still to extents that are acceptable for *in vitro* studies.⁴³ Moreover, a two-way ANOVA analysis indicated that differences in cell viability as a function of exposure time were not significant (P value = 0.0579). Conversely, CS-CL24 PMs were not stable and precipitated very fast. Thus, they were not included in the assay.

PMs are often used as reservoir for the release of the encapsulated drug that is then absorbed in free form. However, in other therapeutic scenarios, they could be capitalized for the passive intracellular delivery of the cargo to phagocytic cells (e.g., macrophages). This is the case of tuberculosis, where alveolar macrophages are the reservoir of the mycobacterium. To evaluate the cellular uptake, HeLa cells, a phagocytic cell line, were incubated with fluorescently-labeled drug-free PMs and the uptake monitored by confocal microscopy (**Figure 11**). The uptake of the PMs (**Figure 11A-C**) was higher than that of a FITC-dextran control (**Figure 11D**) and indicated that the micelles accumulated in the perinuclear region of the cytoplasm. These results also supported the low cytotoxicity of the carriers.

4. CONCLUSIONS

New hybrid drug carriers combining the encapsulation capacity of PMs with the mucoadhesion of CS were extensively investigated. The grafting of oligo(CL) chains onto free-OH moieties of CS was successfully carried out by microwave radiation under relatively mild temperature conditions. It was found that 10 min of irradiation was sufficient to complete the grafting, a remarkable advantage over conventional reactions that require several hours at relatively high temperatures and that usually result in the extensive degradation of the polysaccharide backbone, especially in

acid media. In addition, the reaction conditions were highly reproducible, controllable and with up to 90% higher yields. These new amphiphilic copolymers were soluble several aprotic solvents, unlike their unmodified counterpart CS. Moreover, they were employed for the production of nanoscopic PMs that underwent agglomeration in presence of mucin due to the preservation of free amine groups. Moreover, they allowed the encapsulation of hydrophobic drugs such as the complex RIF to an extent comparable with other micelles that together with mucoadhesion and the capacity to open tight cell junctions constitute advantageous features to prolong and sustain the release of the encapsulated drug in mucosal tissue such as the intestine and the lungs.

ACKNOWLEDGMENTS

RJG and AGM are staff members of CONICET. SQL thanks CONICET for a postdoctoral scholarship. Authors thank the financial support of CONICET (PIP 0220) and the European Union's - Seventh Framework Programme under grant agreement #612675-MC-NANOTAR. MC gratefully acknowledges financial support from the Bundesministerium für Bildung und Forschung (BMBF) through the NanoMatFutur award (13N12561), the Helmholtz Virtual Institute, Multifunctional Biomaterials for Medicine, and the Freie Universität Focus Area Nanoscale. MM acknowledges financial support from the Alexander von Humboldt Foundation. Authors thank Dr. Daniel Vega (CNEA, Argentina), Dr. Pablo Bonelli (Department of Industry, Faculty of Exact Sciences, University of Buenos Aires), Dr. Viviana Campo Dall'Orto (Department of Analytical Chemistry, Faculty of Pharmacy and Biochemistry, University of Buenos Aires) and Dra. Alicia Couto (Department of Organic Chemistry, Faculty of Exact Sciences, University of Buenos Aires,

Argentina) for WAXD, thermal analysis, use of ATR/FT-IR equipment and MALDI-TOF analysis, respectively.

REFERENCES

1. Cabral, H. and Kataoka, K. Progress of Drug-loaded Polymeric Micelles into Clinical Studies. *J. Control. Release* 2014, 190, 465-476.
2. Bromberg, L. Polymeric Micelles in Oral Chemotherapy. *J. Control. Release* 2008, 128, 99-112.
3. Gaucher, G.; Satturwar, P.; Jones, M.-C.; Furtos, A. and Leroux, J.-C. Polymeric Micelles for Oral Drug Delivery. *Eur. J. Pharm. Biopharm.* 2010, 76, 147-158.
4. Mistry, A.; Stolnik, S. and Illum, L. Nanoparticles for Direct Nose-to-Brain Delivery of Drugs. *Int. J. Pharm.* 2009, 379, 146-157.
5. Chiappetta, D.A.; Hocht, C.; Taira, C. and Sosnik, A. Efavirenz-loaded Polymeric Micelles for Pediatric Anti-HIV Pharmacotherapy with Significantly Higher Oral Bioavailability. *Nanomedicine (Lond.)* 2010, 5, 11-23.
6. Chiappetta, D.A.; Hocht, C.; Taira, C. and Sosnik, A. Oral Pharmacokinetics of the Anti-HIV Efavirenz Encapsulated within Polymeric Micelles. *Biomaterials* 2011, 32, 2379-2387.
7. Chiappetta, D.A.; Hocht, C.; Opezzo, J.A.W. and Sosnik, A. Intranasal Administration of Antiretroviral-loaded Micelles for Anatomical Targeting to the Brain in HIV. *Nanomedicine (Lond.)* 2013, 8, 223-237.
8. Moretton, M.A.; Hotch, C.; Taira, C. and Sosnik, A. Rifampicin-loaded 'Flower-like' Polymeric Micelles for Enhanced Oral Bioavailability in an Extemporaneous Liquid Fixed-dose Combination with Isoniazid. *Nanomedicine (Lond.)* 2014, 9, 1635-1650.

9. Xu, L.; Xu, X.; Chen, H. and Li X. Ocular Biocompatibility and Tolerance Study of Biodegradable Polymeric Micelles in the Rabbit Eye. *Colloids Surf. B Biointerfaces* 2013, 112, 30-34.
10. Movassaghian, S.; Merkel, O.M. and Torchilin, V. Applications of Polymer Micelles for Imaging and Drug Delivery. *WIREs Nanomed. Nanobiotechnol.* 2015, in press.
11. Sosnik, A. and Menaker Raskin, M. Muco-adhesive Self-assembly Nanocarriers for Mucosal Drug Delivery: Challenges towards clinical translation. *Biotechnol. Adv.* 2015, in press.
12. Alonso, M.J. and Sanchez, A. The Potential of Chitosan in Ocular Drug Delivery. *J. Pharm. Pharmacol.* 2003, 55, 1451-1463.
13. Zhang, N.; Li, J.; Jiang, W.; Ren, Ch.; Li, J.; Xin, J. and Li, K. Effective protection and controlled release of insulin by cationic β -cyclodextrin polymers from alginate/chitosan nanoparticles. *Int. J. Pharm.* 2010, 393, 212–218.
14. Bian, F.; Jia, L.; Yu, W. and Liu, M. Self-assembled Micelles of *N*-Phthaloylchitosan-g-Polyvinylpyrrolidone for Drug Delivery. *Carbohydr. Polym.* 2009, 76, 454-459.
15. Ifuku, S.; Miwa, T.; Morimoto, M. and Saimoto, H. Preparation of Highly Chemoselective *N*-Phthaloyl Chitosan in Aqueous Media. *Green Chem.* 2011, 13, 1499-1502.
16. Liu, L.; Shi, A.; Guo, S.; Fang, Y.; Chen, S. and Li, S. Preparation of Chitosan-g-Polylactide Graft Copolymers via Self-catalysis of Phthaloylchitosan and Their Complexation with DNA. *React. Funct. Polym.* 2010, 70, 301-305.

17. Duan, K.; Chen, H.; Huang, J.; Yu, J.; Liu, S.; Wang, D. and Li, Y. One-step Synthesis of Amino-reserved Chitosan-*graft*-Polycaprolactone as a Promising Substance of Biomaterial. *Carbohydr. Polym.* 2010, 80, 498-503.
18. Sashiwa, H.; Shigemasa, Y. and Roy, R. Dissolution of Chitosan in Dimethyl Sulfoxide by Salt Formation. *Chem. Lett.* 2000, 29, 596-597.
19. Pramanick, S.; Singodia, D. and Chandel, V. Excipient Selection in Parenteral Formulation Development. *Pharma Times* 2013, 45, 65-77.
20. Woodruff, M.A. and Hutmacher, D.W. The Return of a Forgotten Polymer—Polycaprolactone in the 21st Century. *Prog. Polym. Sci.* 2010, 35, 1217-1256.
21. Moretton, M.A.; Chiappetta, D.A.; Andrade, F.; das Neves, J.; Ferreira, D.; Sarmiento, B. and Sosnik, A. Hydrolyzed Galactomannan-modified Nanoparticles and Flower-like Polymeric Micelles for the Active Targeting of Rifampicin to Macrophages. *J. Biomed. Nanotechnol.* 2013, 9, 1076-1087.
22. Seremeta, K.P.; Chiappetta, D.A. and Sosnik, A. Poly(epsilon-caprolactone), Eudragit® RS 100 and Poly(e-caprolactone)/Eudragit® RS 100 Blend Submicron Particles for the Sustained Release of the Antiretroviral Efavirenz. *Colloids Surf. B Biointerfaces* 2013, 102, 441-449.
23. Duan, K.; Zhang, X.; Tang, X.; Yu, J.; Liu, S.; Wang, D.; Li, Y. and Huang, J. Fabrication of Cationic Nanomicelle from Chitosan-*graft*-Polycaprolactone as the Carrier of 7-Ethyl-10-hydroxy-camptothecin. *Colloids Surf. B Biointerfaces* 2010, 76, 475-482.
24. Glisoni, R.J. and Sosnik, A. Novel Poly(Ethylene Oxide)-*b*-Poly(Propylene Oxide) Copolymer-Glucose Conjugate by the Microwave-Assisted Ring Opening of a Sugar Lactone. *Macromol. Biosci.* 2014, 14, 1639-1651.

25. Giubudagian, M.; Asadian-Birjand, M.; Steinhilber, D.; Achazi, K.; Molina, M. and Calderón, M. Dendritic Polymer Imaging Systems for the Evaluation of Conjugate Uptake and Cleavage. *Polym. Chem.* 2014, 5, 6909-6913.
26. Moretton, M.A.; Glisoni, R.J.; Chiappetta, D.A. and Sosnik, A. Molecular Implications in the Nanoencapsulation of the Anti-tuberculosis Drug Rifampicin within Flower-like Polymeric Micelles. *Colloids Surf. B Biointerfaces* 2010, 79, 467-479.
27. European Pharmacopeia 3rd Edition, Supplement, Council of Europe 2000, 298.
28. Thongborisute, J. and Takeuchi, H. Evaluation of mucoadhesiveness of polymers by BIACORE method and mucin-particle method. *Int. J. Pharm.* 2008, 354, 204-209.
29. Mugabe, C.; Hadaschik, B.A.; Kainthan, R.K.; Brooks, D.E.; So, A.I.; Gleave, M. E. and Burt, H.M. Paclitaxel Incorporated in Hydrophobically Derivatized Hyperbranched Polyglycerols for Intravesical Bladder Cancer Therapy. *BJU Int.* 2009, 103, 978-986.
30. Gotelli, G.; Bonelli, P.; Abraham, G. and Sosnik, A. Fast and Efficient Synthesis of High Molecular Weight Poly(epsilon-caprolactone) Diols by Microwave-assisted Polymer Synthesis. *J. Appl. Polym. Sci.* 2011, 121, 1321-1329.
31. He, Q.; Wu, W.; Xiu, K.; Zhang, Q.; Xu, F. and Li, J. Controlled drug release system based on cyclodextrin-conjugated poly(lactic acid)-*b*-poly(ethylene glycol) micelles. *Int. J. Pharm.* 2013, 443, 110–119.
32. Wang, Z.; Zheng, L.; Li, Ch.; Zhang, D.; Xiao, Y.; Guan, G. and Zhu, W. A Novel and Simple Procedure to Synthesize Chitosan-*graft*-Polycaprolactone in an Ionic Liquid. *Carbohydr. Polym.* 2013, 94, 505-510.
33. Nguyen, S.; Hisiger, S.; Jolicoeur, M.; Winnik, F.M. and Buschmann, M.D. Fractionation and Characterization of Chitosan by Analytical SEC and ¹H NMR after Semi-preparative SEC. *Carbohydr. Polym.* 2009, 75, 636-645.

34. Kalia, S.; Sabaa, M.W. and Kango, S. Polymer Grafting: A Versatile Means to Modify the Polysaccharides. In: Kalia, S. and Sabaa, M.W. (Eds.), Polysaccharide based graft copolymers, Springer-Verlag Berlin Heidelberg 2013, pp. 1-14.
35. Gürdag, G. and Sarmad, S. Cellulose Graft Copolymers: Synthesis, Properties, and Applications. In: Kalia, S. and Sabaa, M.W. (Eds.), Polysaccharide based graft copolymers, Springer-Verlag Berlin Heidelberg 2013, pp. 15-57.
36. Singh, N.K.; Purkayastha, B.D.; Roy, J.K.; Banik, R.M.; Yashpal, M.; Singh, G.; Malik, S. and Maiti, P. Nanoparticle-induced Controlled Biodegradation and Its Mechanism in Poly(ϵ -caprolactone). *ACS Appl. Mater. Interfaces* 2010, 2, 69-81.
37. das Neves, J.; Rocha, C.M.R.; Gonçalves, M.P.; Carrier, R.L.; Amiji, M.; Bahia, M.F. and Sarmiento, B. Interactions of Microbicide Nanoparticles with a Simulated Vaginal Fluid. *Mol. Pharmaceutics* 2012, 9, 3347-3356.
38. Sankar, R.; Sharda, N. and Singh S. Behavior of Decomposition of Rifampicin in the Presence of Isoniazid in the pH range 1-3. *Drug Dev. Ind. Pharm.* 2003, 29, 733-738.
39. Shishoo, C.J.; Shah, S.A.; Rathod, I.S.; Savale, S.S.; Kotecha, J.S. and Shah, P.B. Stability of Rifampicin in Dissolution Medium in Presence of Isoniazid. *Int. J. Pharm.* 1999, 190, 109-123.
40. Pandey, R. and Khuller, G.K. Antitubercular Inhaled Therapy: Opportunities, Progress and Challenges. *J. Antimicrob. Chemother.* 2005, 55, 430-435.
41. Ohashi, K.; Kabasawa, T.; Ozeki, T. and Okada, H. One-Step Preparation of Rifampicin/Poly(lactic-co-glycolic acid) Nanoparticle-Containing Mannitol Microspheres using a Four-fluid Nozzle Spray Drier for Inhalation Therapy of Tuberculosis. *J. Control. Release* 2009, 135, 19-24.

42. He, D.; Deng, P.; Yang, L.; Tan, Q.; Liu, J.; Yang, M. and Zhang, J. Molecular Encapsulation of Rifampicin as an Inclusion Complex of Hydroxypropyl- β -cyclodextrin: Design; Characterization and In Vitro Dissolution. *Colloids Surf. B Biointerfaces* 2013, 103, 580-585.
43. Cavet, M.E.; Harrington, K.L.; VanDerMeid, K.R.; Ward, K.W. and Zhang, J.-Z. Comparison of the Effect of Multipurpose Contact Lens Solutions on the Viability of Cultured Corneal Epithelial Cells. *Cont. Lens Anterior Eye* 2009, 32, 171-175.

Figures legends

Figure 1. Microwave-assisted ring opening grafting of CL to CS templates to amphiphilic copolymers. MSA was used as catalyst, solvent and protectant of side amine groups in CS.

Figure 2. ATR/FT-IR spectrum of (A) pristine CS, (B) CS-CL8 and (C) pristine PCL (M_w of 40 kg/mol). The carbonyl group (C=O) of CL in the graft copolymer was observed at 1726 cm^{-1} .

Figure 3. NMR analysis of CS-CL8 (2%) in acetone- d_6 . (A) ^1H -NMR. The integrals shown for CL and CS at 2.30 and 3.89 ppm, respectively, used to calculate the number of CL units per glucosamine residue. (B) ^{13}C -NMR. The characteristic signal of the newly formed ester bond (C=O) and the methanesulfonate carbon (CH_3SO_3^-) are clearly observed at 174.05 and 40.15 ppm, respectively (indicated with arrows).

Figure 4. (A) MALDI-TOF spectrum and (B) GPC chromatogram of CS-CL8.

Figure 5. DSC thermograms of (A) pristine CS, (B) pristine PCL and (C) CS-CL8 during the second heating ramp. The T_m of pristine PCL and CS-CL8 are indicated with arrows.

Figure 6. TGA thermograms of (A) pristine CS, (B) pristine PCL and (C) CS-CL8.

Figure 7. WAXD diffractograms of pristine CS and PCL, and CS-*g*-oligo(CL) copolymers.

Figure 8. Morphology of RIF-free CS-CL8 PMs (1% w/v) by (A) TEM (scale bar = 100 nm) and (B) AFM (scale bar = $2\ \mu\text{m}$).

Figure 9. TEM micrograph of RIF-loaded CS-CL8 PMs (1% w/v). Scale bar = 50 nm.

Figure 10. Viability of A549 cells exposed to different RIF-free PMs (1% w/v) of CS-CL8, CS-CL12 and CS-CL24 copolymers expressed as relative cell concentration,

as a function of exposure time. The 80-90% of viability was observed up to 24 h post-exposure. A control without treatment was considered 100% viability.

Figure 11. Fluorescent microscopy of HeLa cells exposed (15 h) to: (A) 0.5 mL, (B) 0.1 mL and (C) 0.05 mL of FITC-labeled CS-CL8 PMs and (D) FITC-dextran (control). Green areas represent FITC-labeled PMs, while blue areas represent the DAPI stained nuclei of the cells. Note that PMs seem to accumulate particularly in the perinuclear region.

Tables

Table 1. Weight feeding ratios used for the grafting of CL to pristine CS by microwave-assisted ring opening polymerization and thermal analysis of the copolymers.

Copolymer	CS amount (g)	CL amount (g)	Yield (%)	CL _n ^a	T _m ^b (°C)	ΔH _m ^c (J/g)
CS-CL8	0.5	4.1	75	19.6	50	57.1
CS-CL12		6.2	80	24.3	51	66.2
CS-CL16		8.2	85	32.9	53	70.8
CS-CL24		12.4	90	39.7	54	66.9

^a Experimental average number of CL units per D-glucosamine unit in CS as calculated by ¹H-NMR; ^b melting temperature (T_m) of oligo(CL) blocks determined during the second heating ramp and ^c enthalpy of fusion (ΔH_m) of oligo(CL) blocks determined during the second heating ramp and normalized to the oligo(CL) content.

Table 2. Experimental M_w of the different copolymers determined by MALDI-TOF and GPC.

Copolymer	MALDI-TOF MS ^a			GPC	
	M _w (g/mol)			M _w (g/mol)	M _w /M _n
	Fraction 1	Fraction 2	Fraction 3		
CS-CL8	1067.5 (611.3-1751.9)	2550.4 (1751.9-3918.9)	5176.3 (3918.9-5747.2)	2960	1.7
CS-CL12	1067.4 (611.2-2094.1)	2550.3 (2094.1-4146.9)	5062.3 (4146.9-5744.5)	6140	3.8
CS-CL16	953.4 (611.0-1865.9)	2550.4 (1865.9-4375.0)	5175.3 (4375.0-6314.7)	2690	2.0
CS-CL24	1173.9 (611.3-2116.4)	2544.0 (2116.4-4147.0)	5176.7 (4147.0-6658.1)	3700	2.5

^a MALDI-TOF MS showed three *m/z* populations. Values presented in the table correspond to the peak maxima of each fraction. The *m/z* range for each fraction is indicated between brackets.

Table 3. Characterization of the micellization process and the RIF-free and RIF-loaded PMs at 37°C.

Copolymer	RIF-free PMs				RIF-loaded PMs				Mucoadhesion		
	CMC (10 ⁻⁴ % w/v)	D _h ^a (nm) (± S.D.)	PDI	Z-potential (mV) (± S.D.)	RIF cargo ^b (mg/mL) (± S.D.)	%RIF ^c (± S.D.)	%EE ^d (± S.D.)	f _s (± S.D.)	D _h ^e (nm) (± S.D.)	MI	D _h ^f (nm) (± S.D.)
CS-CL8	3.6	110.7 (2.4)	0.13 (0.02)	+53.0 (0.8)	3.57 (0.05)	26 (0.2)	36 (0.5)	1.7 (0.02)	118.0 (2.1)	3.4	483.2 (19.9)
CS-CL12	3.7	115.6 (2.0)	0.21 (0.03)	+54.2 (0.7)	3.12 (0.27)	24 (1.6)	31 (2.8)	1.5 (0.13)	121.6 (2.0)	6.5	548.8 (10.3)
CS-CL16	4.9	121.7 (5.5)	0.23 (0.05)	+53.4 (0.8)	3.96 (0.37)	28 (1.9)	40 (3.7)	1.9 (0.17)	126.0 (4.7)	9.2	902.3 (8.2)
CS-CL24	5.0	153.7 (5.2)	0.12 (0.02)	+54.5 (0.6)	ND	ND	ND	ND	ND	ND	ND

^a Hydrodynamic diameter (D_h) of drug-free CS-*g*-oligo(CL) PMs (1% w/v), determined by DLS; ^b RIF cargo in 1% w/v PMs; ^c RIF loading (%RIF) considering the concentration of copolymer in the system; ^d Encapsulation efficiency of RIF (%EE) calculated based on the total amount of RIF included in the encapsulation stage; f_s, Solubility factor, defined as S_{PM}/S_{water} where, S_{PM} is the solubility of RIF within PMs and S_{water} the intrinsic solubility of RIF water at 25°C; ^e Hydrodynamic diameter (D_h) of RIF-loaded CS-*g*-oligo(CL) PMs (1% w/v), determined by DLS; MI, Mucoadhesion index, defined as D_{h2}/D_{h0} where, D_{h0} and D_{h2} represent the values of D_h before (t = 0 hours) and after (t = overnight) incubation with mucin (0.25% w/v) at 37°C, respectively; ^f Hydrodynamic diameter (D_h) reached after the incubation with mucin (0.25 % w/v) at 37°C, determined by DLS; ND: Not determined because of the poor solubility of RIF-loaded 1:24 CS-*g*-oligo(CL) derivative at 1% w/v in water.

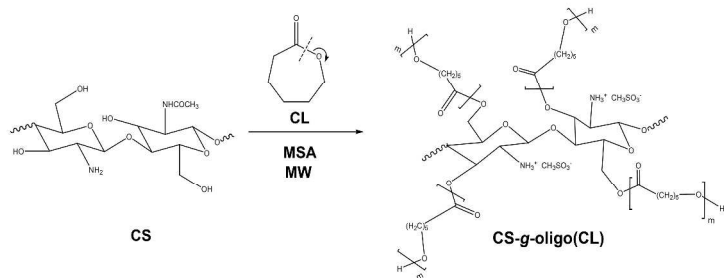


Figure 1. Microwave-assisted ring opening grafting of CL to CS templates to amphiphilic copolymers. MSA was used as catalyst, solvent and protectant of side amine groups in CS.
2079x838mm (96 x 96 DPI)

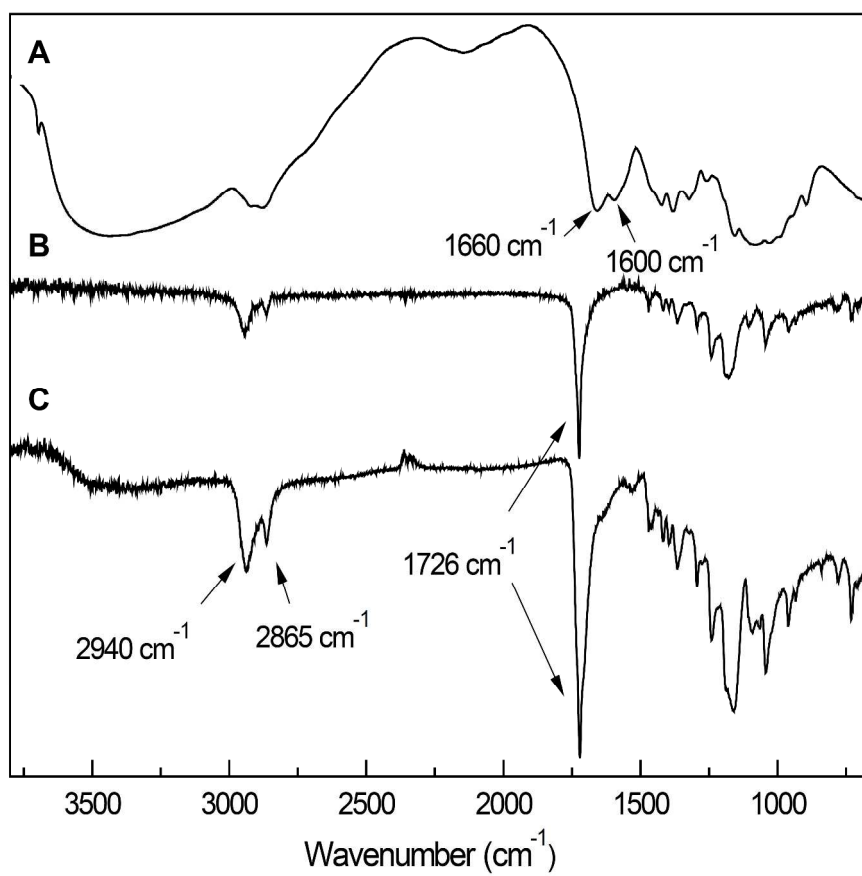


Figure 2. ATR/FT-IR spectrum of (A) pristine CS, (B) CS-CL8 and (C) pristine PCL (MW of 40 kg/mol). The carbonyl group (C=O) of CL in the graft copolymer was observed at 1726 cm^{-1} .
1087x962mm (96 x 96 DPI)

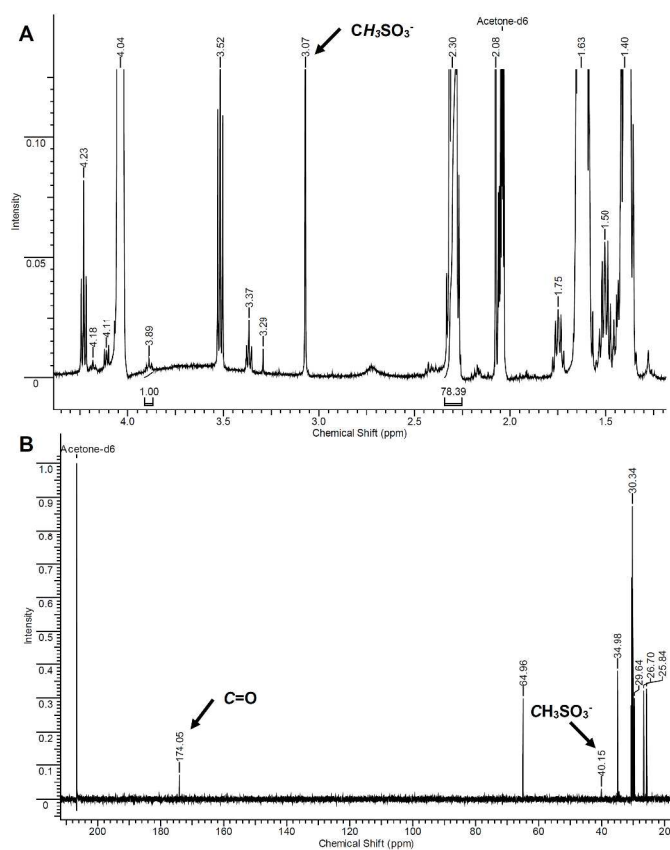


Figure 3. NMR analysis of CS-CL8 (2%) in acetone-d₆. (A) ¹H-NMR. The integrals shown for CL and CS at 2.30 and 3.89 ppm, respectively, used to calculate the number of CL units per glucosamine residue. (B) ¹³C-NMR. The characteristic signal of the newly formed ester bond (C=O) and the methanesulfonate carbon (CH₃SO₃⁻) are clearly observed at 174.05 and 40.15 ppm, respectively (indicated with arrows).

1087x933mm (96 x 96 DPI)

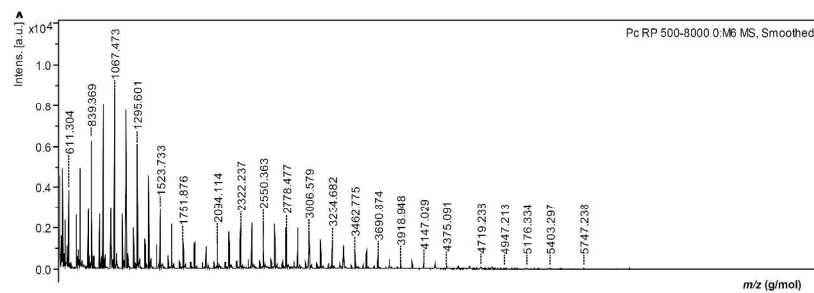


Figure 4A. MALDI-TOF spectrum of CS-CL8.
1087x797mm (96 x 96 DPI)

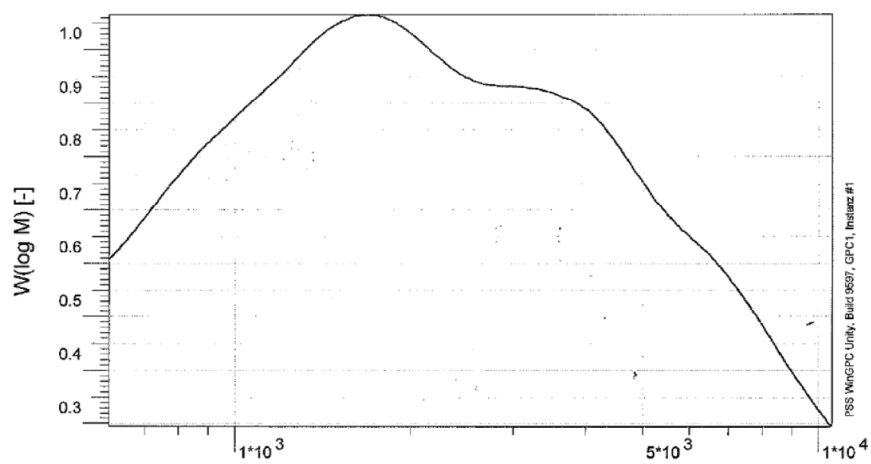


Figure 4B. GPC chromatogram of CS-CL8.
761x558mm (96 x 96 DPI)

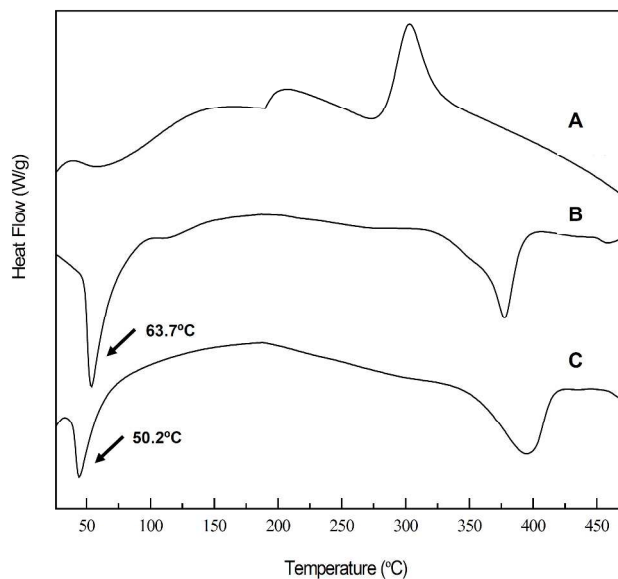


Figure 5. DSC thermograms of (A) pristine CS, (B) pristine PCL and (C) CS-CL8 during the second heating ramp. The T_m of pristine PCL and CS-CL8 are indicated with arrows.
1087x797mm (96 x 96 DPI)

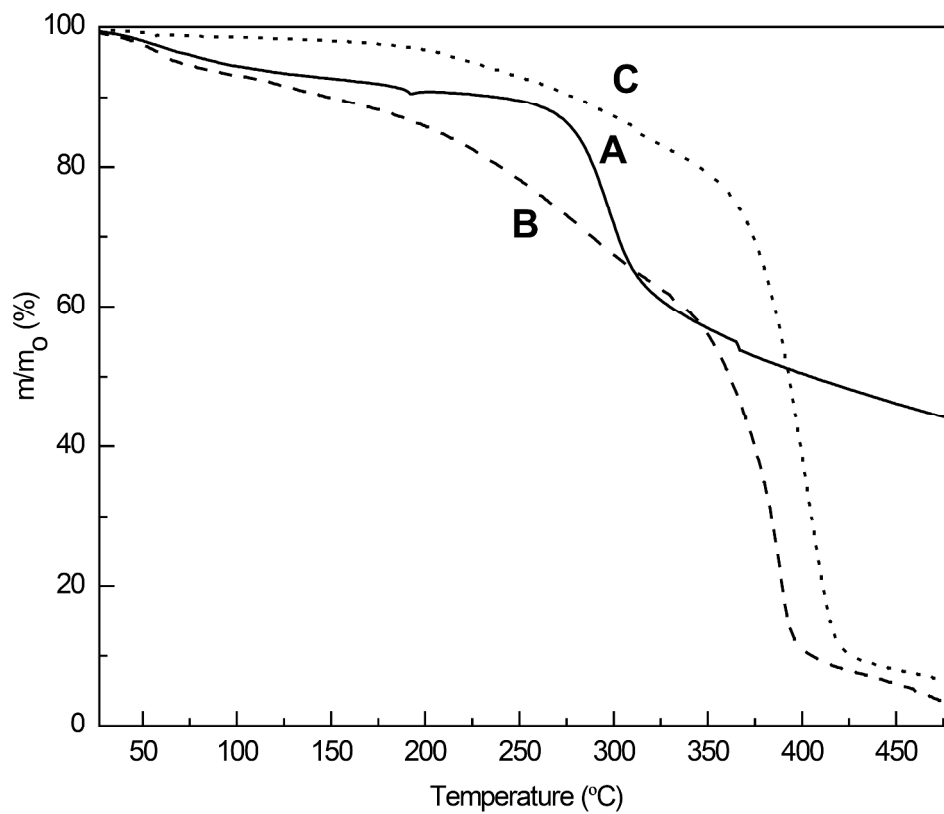


Figure 6. TGA thermograms of (A) pristine CS, (B) pristine PCL and (C) CS-CL8.
1376x1142mm (96 x 96 DPI)

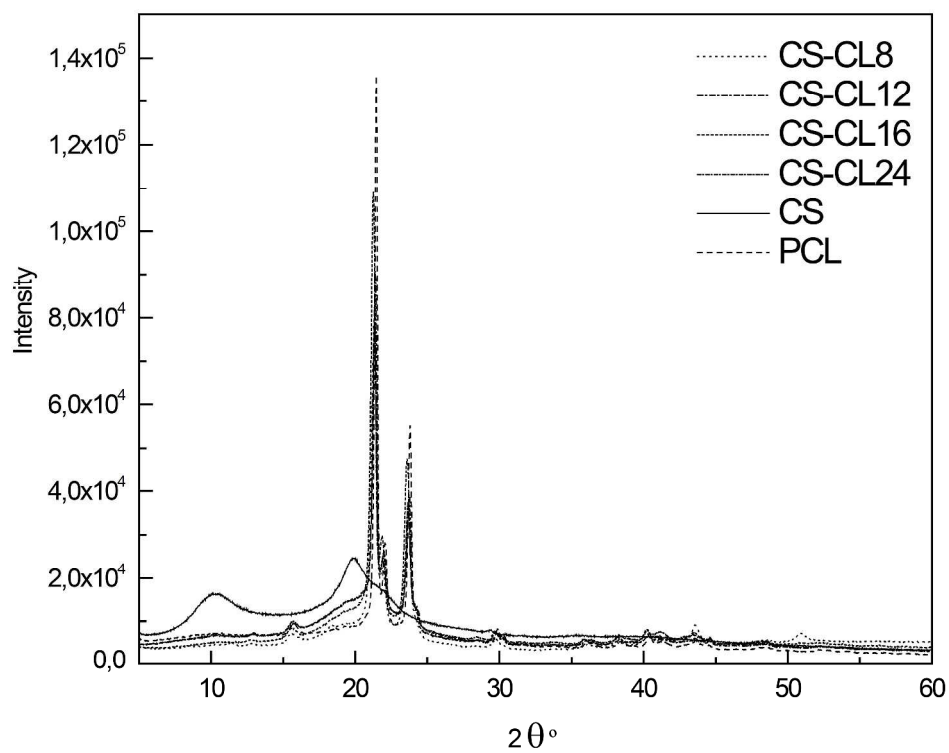


Figure 7. WAXD diffractograms of pristine CS and PCL, and CS-g-oligo(CL) copolymers.
1404x1062mm (96 x 96 DPI)

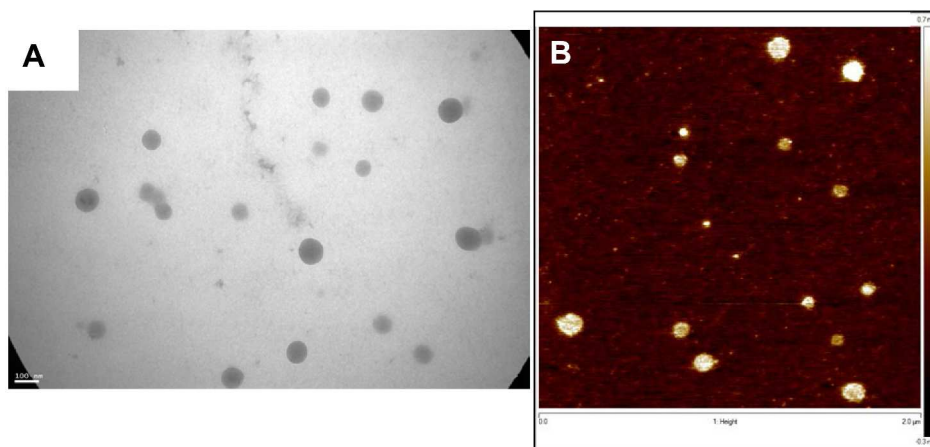


Figure 8. Morphology of RIF-free CS-CL8 PMs (1% w/v) by (A) TEM (scale bar = 100 nm) and (B) AFM (scale bar = 2 μ m).
1659x814mm (96 x 96 DPI)

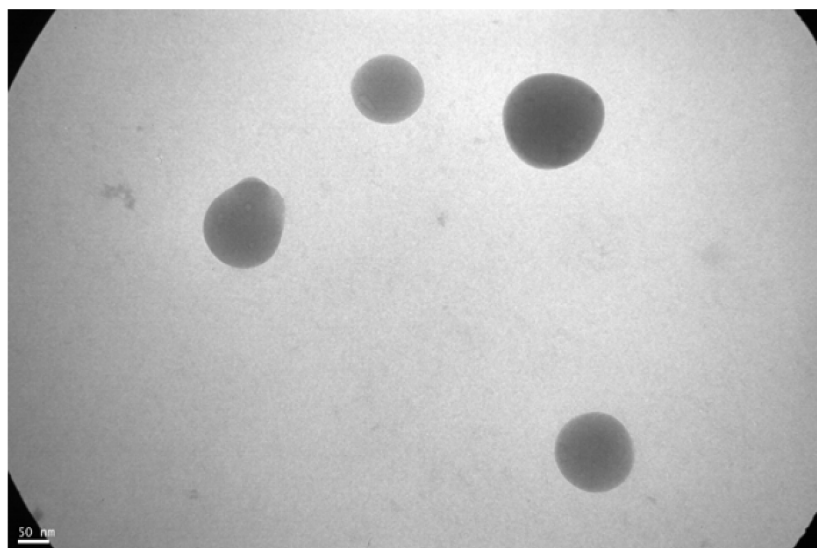


Figure 9. TEM micrograph of RIF-loaded CS-CL8 PMs (1% w/v). Scale bar = 50 nm.
1087x797mm (96 x 96 DPI)

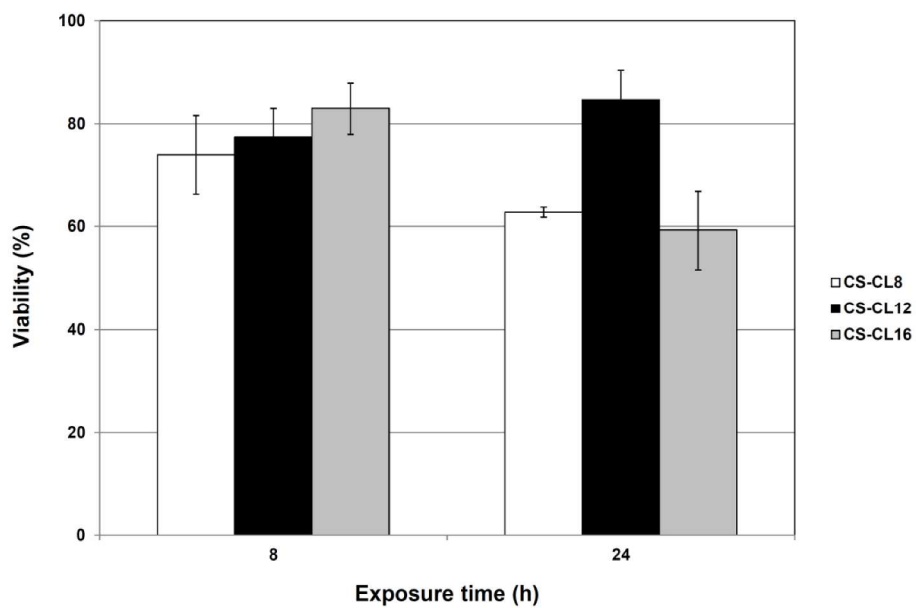


Figure 10. Viability of A549 cells exposed to different RIF-free PMs (1% w/v) of CS-CL8, CS-CL12 and CS-CL24 copolymers expressed as relative cell concentration, as a function of exposure time. The 80-90% of viability was observed up to 24 h post-exposure. A control without treatment was considered 100% viability.
1087x797mm (96 x 96 DPI)

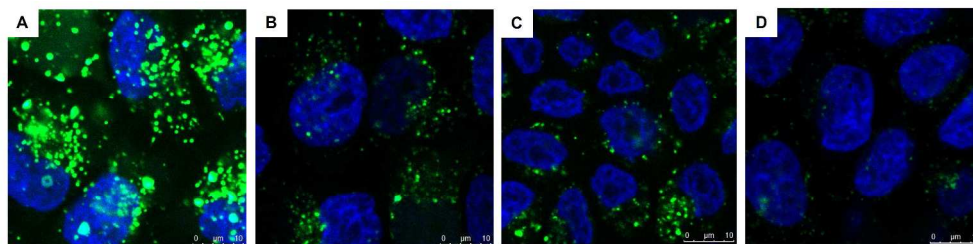


Figure 11. Fluorescent microscopy of HeLa cells exposed (15 h) to: (A) 0.5 mL, (B) 0.1 mL and (C) 0.05 mL of FITC-labeled CS-CL8 PMs and (D) FITC-dextran (control). Green areas represent FITC-labeled PMs, while blue areas represent the DAPI stained nuclei of the cells. Note that PMs seem to accumulate particularly in the perinuclear region.

1171x797mm (96 x 96 DPI)